Solar Cells, *17* (1986) 253–274

SOLAR CELL EFFICIENCY MEASUREMENTS

K. A. EMERY and C. R. OSTERWALD

Solar Energy Research Institute, 1617 Cole Blvd., Golden, CO 80401 (U.S.A.)

(Received August 2, 1985; accepted August 2, 1985)

Summary

The calibration and efficiency measurement procedures followed by the PV Devices and Measurements Branch at the Solar Energy Research Institute (SERI) are presented. The use of spectral irradiance measurements to calibrate reference cells used in these measurements has reduced the uncertainty in the calibration number to less than 1%. The use of the spectral mismatch index can reduce the errors in short-circuit current measurements to about 2% for a wide variety of test cell/reference cell combinations and reduce the need for a close match between the test cell and reference cell spectral responses or the source spectrum and standard spectrum. The effect of various spectra in use by the PV community on the short-circuit current is presented for a variety of cell spectral responses.

1. Introduction

The need for meaningful performance comparisons of different photovoltaic (PV) devices has given rise to efficiency measurements performed under standard solar spectral irradiance and test conditions. The photovoltaic conversion efficiency, which is determined from the current *versus* voltage (*I–V*) characteristics of an illuminated cell, is typically measured with respect to a standard solar spectrum at a given intensity (100 mW cm^{-2}). Several different standard spectra are in use by the PV community [1–6]. These spectra represent direct normal [1, 2, 4, 5] and global irradiation [3, 5, 6] under different atmospheric conditions. Several investigators have proposed measuring the PV performance over a period of time and reporting an energy rating based on a large number of measurements [7]. Although these energy rating methods do not provide information on the efficiency with respect to a standard solar spectrum, they do provide information on the field performance over extended time periods under varying site specific solar insolation conditions. This report will discuss the issues associated

0379-6787/86/$3.50

with measuring the efficiency with respect to a standard solar spectrum under standard test conditions, and the specific procedures followed by the SERI PV Devices and Measurements Branch will be presented.

The efficiency η of a PV device expressed as a percentage is defined [1] as

$$\eta = \left(\frac{\text{Maximum Electrical Power}}{\text{Area} \times \text{Irradiance}} \right) \times 100 = \frac{P_{\max}}{A \times E_{\text{STND}}} \times 100 \tag{1}$$

where A is the total area defined in Appendix A, $P_{\max}$ is the maximum power and E_{STND} is the irradiance of the standard spectrum normalized to some total irradiance. A brief review of the history of standard reporting conditions, *i.e.* temperature, intensity and spectrum, for solar cell efficiency measurements is given in Appendix B. The total irradiance E_{STND} is normally 100 mW cm^{-2} although all of the standard spectra currently employed have a total irradiance of less than 100 mW cm^{-2}. For a meaningful and accurate measurement of η, the irradiance is measured with a reference cell whose short-circuit current is calibrated with respect to a standard spectrum (the calibration procedure used by the PV D & M Branch at SERI is discussed in the following section). The efficiency of a PV device is normally measured in a solar simulator using the reference cell method where the simulator intensity is adjusted so that the measured short-circuit current of the reference cell is equal to its calibrated value at the standard test intensity (100 mW cm^{-2}). This procedure can also be used outdoors where the reference cell measures the intensity. Since the outdoor intensity will not equal 100 mW cm^{-2} an error in the voltage will occur. The current varies approximately linearly with intensity; hence, the error in the current due to intensity can be corrected. The reference cell method will introduce an error in the current and hence η due to a spectral mismatch between the source spectrum (simulated or natural sunlight) and a standard spectrum and between the spectral response of the reference cell and device under test. The methodology to correct the current for these spectral mismatch errors is discussed in Appendix C.

2. Calibration of reference cells

A variety of procedures has been adopted to calibrate reference cells with respect to a standard solar spectrum [1, 6, 8–11]. The method used in calibrating the reference cells at SERI (similar to ref. 10) is believed to give the lowest absolute uncertainty of the various methods and allows for calibrating with respect to different standard spectra.

The calibration number *CN* of a solar cell illuminated by a given standard solar spectral irradiance can be defined as

$$CN_{STND} = \frac{\int_0^\infty E_{STND}(\lambda)\, SR(\lambda)\, d\lambda}{\int_0^\infty E_{STND}(\lambda)\, d\lambda} \tag{2}$$

where $E_{STND}(\lambda)$ is a given standard solar spectral irradiance and $SR(\lambda)$ is the absolute spectral response of the solar cell. When measured outdoors, CN can be written as

$$CN = \frac{I_{sc}}{E_{TOT}} = \frac{\int_0^\infty E_S(\lambda)\, SR(\lambda)\, d\lambda}{\int_0^\infty E_S(\lambda)\, d\lambda} \tag{3}$$

where I_{sc} is the cell short-circuit current, E_{TOT} is the total integrated solar irradiance, and $E_S(\lambda)$ is the measured incident solar spectral irradiance. Equation (3) can be arranged so that

$$1 = \frac{I_{sc} \int_0^\infty E_S(\lambda)\, d\lambda}{E_{TOT} \int_0^\infty E_S(\lambda)\, SR(\lambda)\, d\lambda} \tag{4}$$

Using eqn. (4) in eqn. (2) and integrating over finite limits gives

$$CN_{STND} = \frac{I_{sc} \int_a^b E_{STND}(\lambda)\, SR(\lambda)\, d\lambda \int_a^b E_S(\lambda)\, d\lambda}{E_{TOT} \int_a^b E_{STND}(\lambda)\, d\lambda \int_a^b E_S(\lambda)\, SR(\lambda)\, d\lambda} \tag{5}$$

If I_{sc}, E_{TOT}, and $E_S(\lambda)$ are measured simultaneously with the same field of view (FOV), and if $SR(\lambda)$ can be measured, then the calibration number with respect to $E_{STND}(\lambda)$ can be obtained. Wavelength-invariant bias errors associated with $E_S(\lambda)$ and $SR(\lambda)$ drop out of eqn. (5) and do not affect CN_{STND}. In calculating the calibration number using eqn. (5) it is assumed

that $E_{STND}(\lambda)$ is zero outside the given limits. Equation (5), which can be applied to direct beam or global conditions provides a method of calibrating solar cells with respect to an arbitrary $E_{STND}(\lambda)$. The total irradiance E_{TOT} is measured with a cavity radiometer model MK VI (Technical Measurements Inc., Kendall) with an FOV of 5.0°. The cavity radiometer is used rather than a global irradiance pyranometer (*i.e.* 180° FOV) because its accuracy is at least an order of magnitude less (± 0.5% *versus* ± 5%)[12] and the field of view can be more easily controlled. The power density measured by the cavity radiometer outdoors under natural sunlight should be neglible for $\lambda < a$ and $\lambda > b$ to prevent errors in eqn. (5). The error is less than 0.3% for $a = 0.3$ μm and $b = 4.0$ μm [13]. The short-circuit current is measured with a 0.1 Ω 0.1% accurate four-terminal resistor [14], and the cell voltage at I_{sc} is kept less than ± 1 mV using a bipolar power supply, while the device temperature is kept at 28 ± 1 °C. an HP 85 computer simultaneously triggers the voltmeters used to measure I_{sc} and E_{TOT}. Four baffled collimating tubes are used to match the cavity radiometer field of view [15] so that four cells can be calibrated at the same time. The spectral responses of the cells are measured in the laboratory using a narrow bandwidth (~10 nm) interference filter system with a resolution of 20 nm in the visible and 50 nm in the infrared. The solar spectral irradiance ($E_S(\lambda)$) is measured using a model LI-COR LI-1800 spectroradiometer (range 0.38-1.1 μm, bandwidth 6 nm, FOV = 5.7°). Spectral data for the ranges 0.30-0.38 μm and 1.1-4.0 μm are generated with a direct normal computer model fit to the LI-COR spectra [16]. The extension of $E_S(\lambda)$ to the wavelength range 0.3-4.0 μm is essential to prevent CN_{STND} in eqn. (5) from being ~23% low. Measurement of each LI-COR spectrum requires about 50 s. During this time the calibration number (I_{sc}/E_{TOT}) is sampled at discrete times and averaged to produce one uncorrected calibration number; data taken during any conditions of solar instability greater than 1% were not included in the calibration. The integrations in eqn. (5) are performed using a trapezoidal numerical integration routine. Some results of the calibration of several reference cells are summarized in Appendix D.

3. Efficiency measurement instrumentation and procedures

A block diagram of the basic current *versus* voltage (*I-V*) system is shown in Fig. 1. The variable load can be either of a voltage ramp, variable power supply or load resistors. The use of a voltage ramp is most convenient because once the ramp rate, initial and final voltages are set, the *I-V* measurement can be initiated by pressing a single button. A variable power supply can be useful in rapidly measuring the short-circuit current I_{sc}, maximum power point P_{max} or the current at a given voltage. Load resistors are not recommended for cell evaluation because I_{sc} is never exactly reached and the reverse bias characteristic cannot be determined although the use of load resistors to evaluate the performance of a module or panel

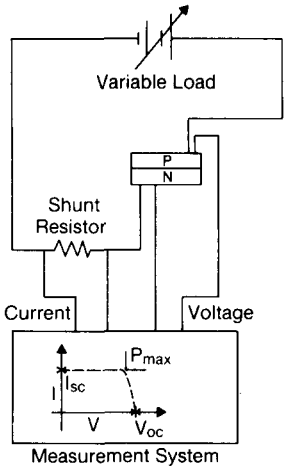

Fig. 1. Block diagram for manual current *vs.* voltage measurement system.

can provide an inexpensive means of determining the performance near P_{max} and I_{sc}.

The current through the cell is monitored with a shunt resistor, electrometer or a feedthrough current transducer. A shunt resistor is the most common method of measuring the current and uses a voltmeter, *X-Y* recorder, or analog to digital (A/D) converter with a computer to measure the voltage across the resistor. Most *I-V* systems use a four-terminal shunt resistor. If a two-terminal resistor is used then the voltage sense wires should be connected as close as possible to the resistor and the resistance measured with a four-terminal ohm meter. It should be noted that any error in the value of the resistance translates directly into an error in the measured current. The power rating on the shunt resistor should be much larger than the square of the maximum current that the system is designed to handle multiplied by the value of the shunt resistor. This will prevent errors from being introduced by the resistor heating. The temperature coefficient of the resistor should be as low as possible to prevent errors arising from different ambient temperatures. The value of the shunt resistor should be chosen so that the voltage across the shunt is $\leqslant 100$ mV. This will allow the voltage across the variable load to remain close to the voltage across the cell making the power supply bias and current range less critical. If the voltage across the shunt resistor is small, then resistor noise can become significant and introduce errors in the current measurement. These errors would tend to predict a greater current than is actually flowing through the cell. The choice of a voltmeter, *X-Y* recorder or an A/D converter to measure the voltage across the shunt resistor is dependent on the resolution, accuracy and speed desired. A voltmeter is the most accurate and an *X-Y* recorder the least accurate while an A/D converter is the fastest. The use of an electrometer is warranted if the system is required to measure currents

below 10 μA. Several investigators have used a current transducer because it is easy to use and does not load the circuit. The use of a current transducer is limited to a narrow current range and may give misleading values if not properly used.

The voltage across the cell is easily measured with any high impedance voltmeter or X-Y recorder. The limiting uncertainty in the voltage measurement is the ability to monitor and control the junction temperature accurately. Near the maximum power point uncertainties in the voltage can exist due to the contacting method.

The measurement of P_{max} can be performed manually by monitoring the product of the voltage and current. Constant power curves overlaid on an I-V plot produced by an X-Y recorder can also be used or the I-V curve can be digitized near the maximum power point to determine the voltage and current P_{max}. These graphical methods are limited by the width of the line producing the I-V curve and the operator's ability to set the zero and determine P_{max}. Analog circuits have been developed to track the maximum power point of cells, modules or arrays. While the accuracy of these circuits is limited by their ability to "home" in on P_{max} in the presence of fluctuations in the current, these circuits can usually locate P_{max} to within 1% which is acceptable for arrays or modules, but may not be acceptable for devices.

A wide variety of automated I-V test systems have been built to suit a range of needs. Several papers have been published describing automated I-V measurements [17-20]. These systems are characterized by a digital to analog (D/A) converter (computer controlled power supply) to replace the variable load (manual power supply) in Fig. 1 and utilize A/D conversion to monitor the voltage across the cell and the shunt resistor. Automated systems offer graphical and tabular presentation of the data in addition to data storage [17-20] and are capable of correcting the illuminated current for fluctuations in the light intensity about a set value which can achieve ±0.1% repeatability in the current, a capability manual I-V systems do not have.

The I-V measurement system currently in use in the PV D & M Branch at SERI shown in Fig. 2 is capable of manual or automatic measurements over the current range of $\pm 10^{-10}$ A to ± 8 A, with a voltage range of ± 50 V. For automatic tests, the system is controlled by an HP1000F computer which also stores the data on hard disc and produces graphical outputs.

Figure 2 shows the test system configured for I-V measurements in a slightly simplified manner. Four-terminal contacts are made to the test cell whose temperature is controlled by a thermoelectric temperature controller which allows a −50 to +100 °C temperature variation. One top and one bottom contact is connected to an HP3456A digital voltmeter and thus measures the cell terminal voltage. The HP3456A can measure 1 μV d.c. but uncertainties in the intensity and temperature limit the resolution to about 100 μV. Another HP3456A is used to monitor the current through the intensity monitor cell which is used for correction of the test cell current

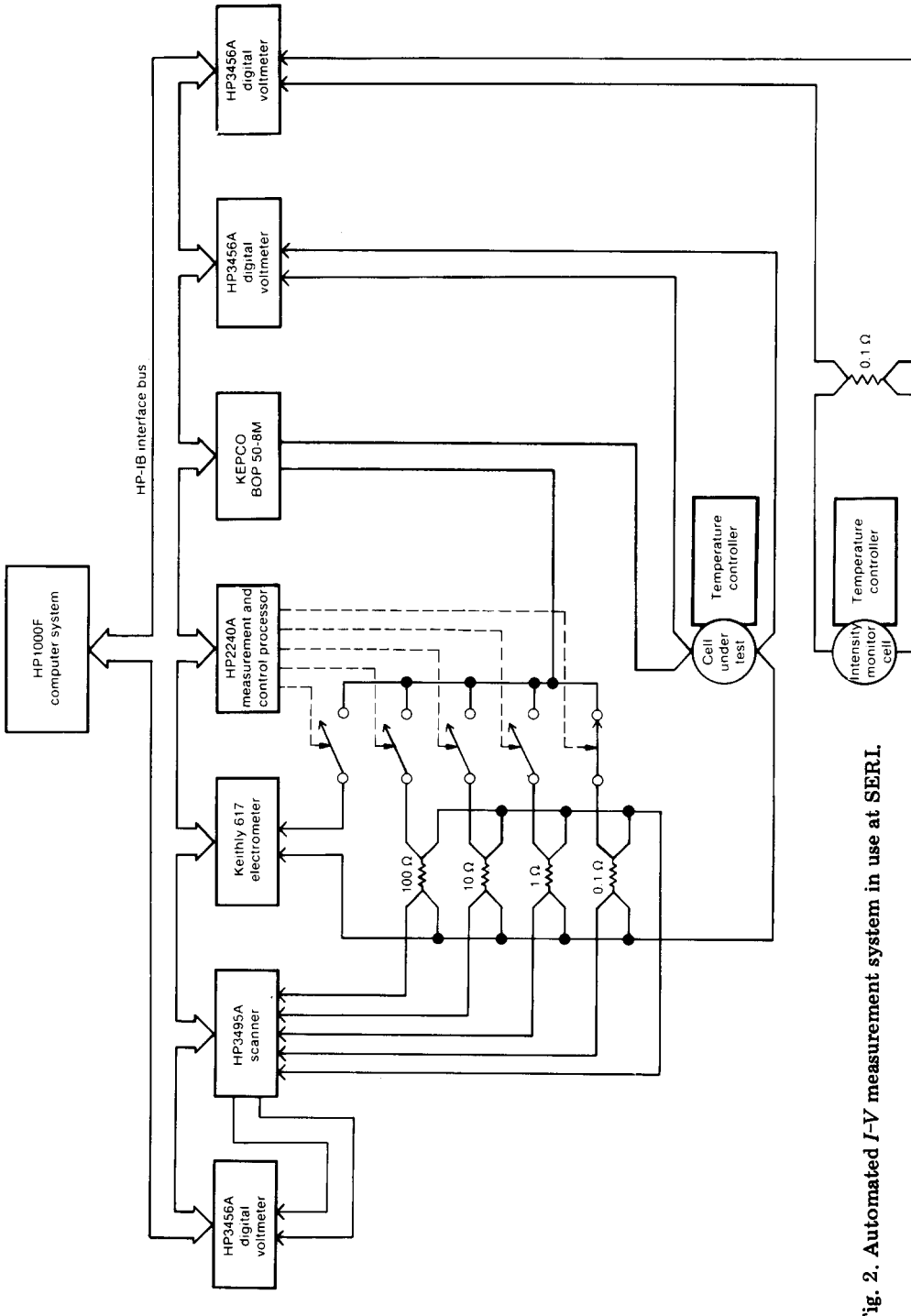

Fig. 2. Automated *I–V* measurement system in use at SERI.

to a constant intensity value. A separate temperature controller for the intensity monitor allows the temperature of the test cell to be varied without affecting the current calibration of the intensity monitor.

Because the test cell current can vary over ten orders of magnitude, five current ranges are used which are selected with the HP2240A Measurement and Control Processor. Four of these are precision four-terminal resistors arranged in decades from 0.1 to 100 Ω for current measurements from 8 A to 10^{-5} A. The voltage across these resistors is measured by a third HP3456A with the proper connection made by an HP3495A scanner. Low-current measurements are made with a Keithly 617 electrometer. Cell V_{oc} is measured by opening the current loop relays and measuring the cell voltage.

Cell bias is accomplished with a KEPCO BOP50-8M programmable bipolar power supply which is capable of ±1 mV resolution in the ±5 V range and ±10 mV in the ±50 V range.

Other features of the system not shown in Fig. 2 include the ability to measure the resistance in the top or bottom contact pair of the test cell with the cell bias voltmeter set to two-terminal resistance. This allows detection of high contact resistance problems which can yield low fill factor. The

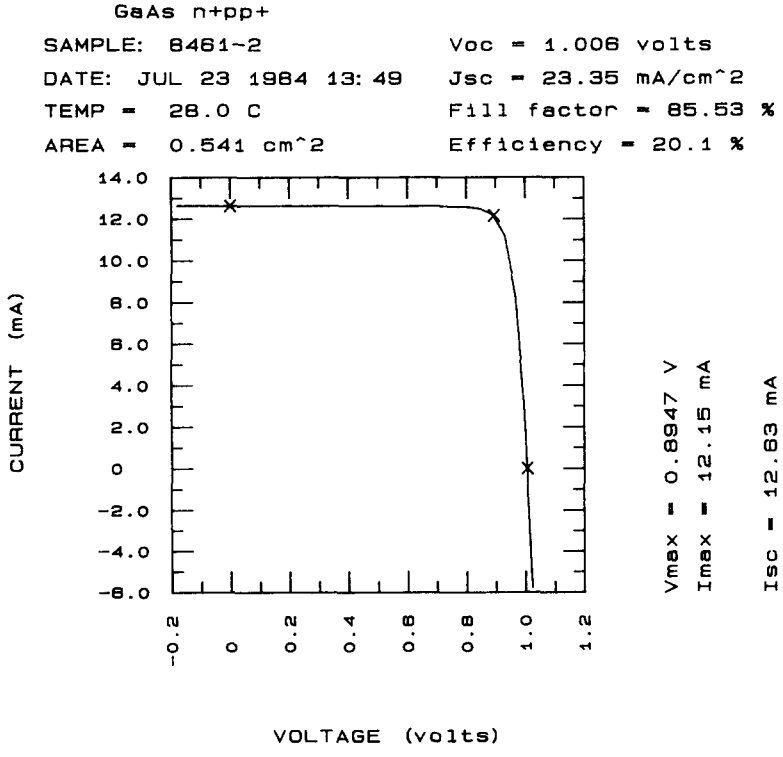

Fig. 3. Graphical output from the SERI PV D & M automated *I-V* system showing the illuminated *I-V* characteristics of a high efficiency solar cell with respect to standard test conditions.

HP3456A voltmeters and the electrometer are triggered simultaneously for each reading which assures that at each bias point the data is taken during the same time frame for each instrument. This is especially important in reducing errors in I_{sc} due to intensity fluctuations in the solar simulator.

The procedure employed in the PV D & M Branch at SERI for measuring the efficiency of PV devices is summarized. Upon receipt of a cell, the total area is measured using the definition in Appendix A. The spectral response is measured to determine the appropriate reference cell and the spectral mismatch index discussed in Appendix C is computed. The intensity of the Spectrolab X-25 solar simulator (see Fig. C1 for a typical spectrum) is adjusted to 100 mW cm^{-2} using a reference cell followed by calibrating the intensity monitor. The test cell is then mounted in the simulator test plane and the temperature adjusted to give a cell temperature of 28 ± 0.1 °C (25 °C). Four-terminal contact is then made to the device and the contact resistance between the voltage and current contacts is minimized (< 3 Ω). The computer program used to measure the efficiency is then executed; which prompts the user for a title, the sample number, cell area, intensity, temperature and intensity monitor calibration current. The measurement system then measures the open-circuit voltage V_{oc} and determines the base type. Using this information, the computer biases the cell from $V_{oc}(1 + 1/30)$

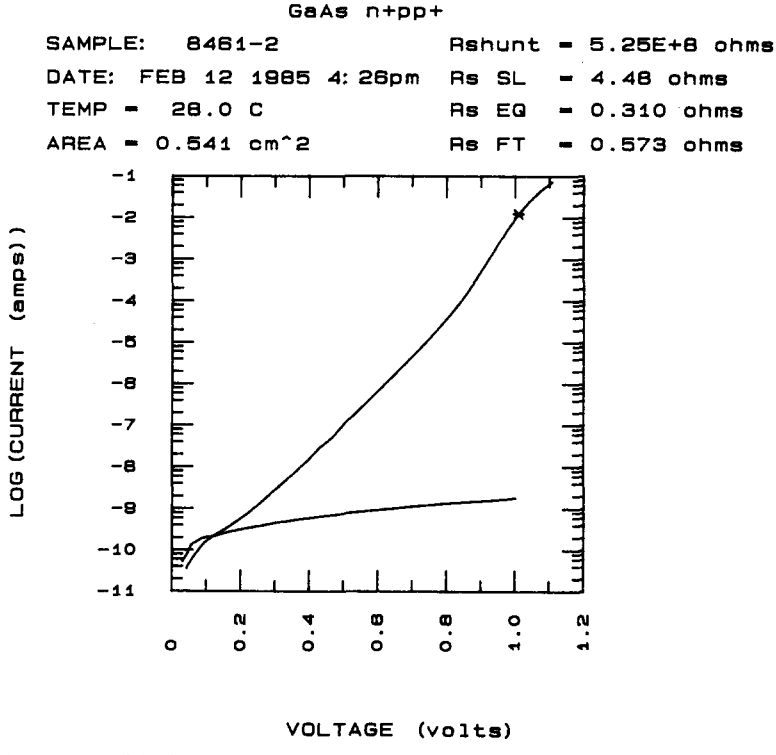

Fig. 4. Graphical output from the SERI PV D & M dark *I-V* measurement system.

in forward bias to 200 mV in reverse bias at discrete points, correcting the current at each point for intensity fluctuations.

A separate high resolution maximum power algorithm is used to locate the maximum power point within ± 2 mV. The short-circuit current is obtained by adjusting the bias until the voltage across the cell is less than 2 mV. Once the measurement is completed, the illuminated *I-V* parameters are displayed and can then be stored and plotted. The measured short-circuit current is then corrected for spectral mismatch as described in Appendix C. An alternative procedure is to correct the short-circuit current of the reference cell ($CN_{STND} \times 100$ mW cm^{-2}) for spectral mismatch, thereby setting the simulator to the proper intensity and correcting the current over the entire voltage range for spectral mismatch errors.

An example of the illuminated *I-V*, dark *I-V*, and quantum efficiency characteristics of a high efficiency GaAs/GaAlAs solar cell are given in Figs. 3-6. The illuminated *I-V* characteristics in Fig. 3 were measured under standard test conditions at 28 °C, 100 mW cm^{-2} with respect to the direct normal spectrum in Table B1. The dark *I-V* characteristics for this cell are given in Fig. 4; while the absolute quantum efficiency as a function of wavelength of this cell with and without a light bias is given in Figs. 5 and 6

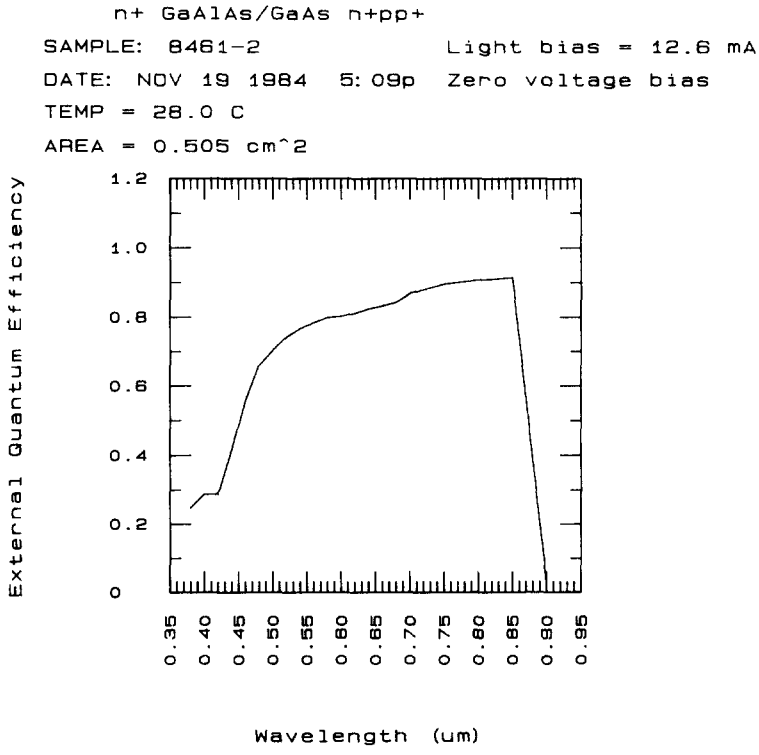

Fig. 5. Graphical output from the SERI PV D&M spectral response measurement system with light bias.

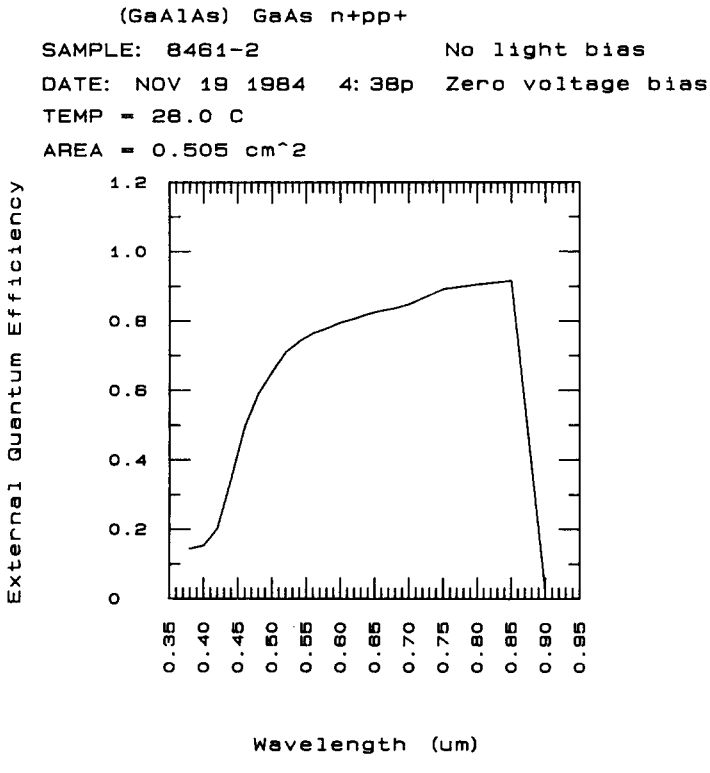

Fig. 6. Graphical output from the SERI PV D & M spectral response measurement system without light or voltage bias.

respectively. The intensity of the tungsten halogen bias light was adjusted to give the short-circuit current under standard test conditions, *i.e.* 12.6 mA. Using the quantum efficiency data in Fig. 5 and the GaAs reference cell SO2 in Fig. D2 with the spectrum in Table 1 and Spectrolab X-25 spectral irradiance in Fig. C1 gives a spectral mismatch M of 1.009, while the quantum efficiency data in Fig. 6 gives an M of 1.002. The data in Fig. 3 were not corrected for the $< 1\%$ error in spectral mismatch.

4. Conclusion

The PV Devices and Measurements Branch's efficiency measurement systems and test procedures are designed to minimize the error in measurement with respect to selected standard test conditions. The effect of various direct and global standard spectra on the calibration number are compared. The use of the spectral mismatch index to correct for differences between the source and standard spectrum and the test and reference cell spectral response has reduced the errors in I_{sc} to below 2% for indoor or outdoor measurements. The spectral mismatch correction of indoor measurements is more accurate than uncorrected outdoor PV measurements.

Acknowledgments

The authors wish to acknowledge Roland Hulstrom, Ted Cannon and Daryl Meyers for assistance in making the spectral measurements and helpful comments, Russ Hart at NASA Lewis Research Center for supplying reference cells and technical support, L. L. Kazmerski for his support and encouragement, and Pat Newman for typing the manuscript. This work was supported by the U.S. Department of Energy under contract DE-AC02-83H10093.

References

1 Terrestrial photovoltaics measurement procedures, *NASA Tech. Memo. TM 73702*, National Aeronautics and Space Administration, Cleveland, OH, 1977.
2 Terrestrial direct normal solar spectral irradiance tables for air mass 1.5, *ASTM Std. E891*, American Society for Testing and Materials, 1916 Race Street, Philadelphia, PA, 1982.
3 Terrestrial solar spectral irradiance tables at air mass 1.5 for a 37° tilted surface, *ASTM Std. E892*, American Society for Testing and Materials, 1916 Race Street, Philadelphia, PA, 1982.
4 R. Shimokawa, K. Fujisaw, M. Horiguchi, S. Yoshikawa and Y. Hamakawa, *Proc. 5th Commission of the European Communities Conf. on Photovoltaic Solar Energy, Athens, Greece, October 17–21, 1983*, Reidel, Dordrecht, 1983, pp. 657–661.
5 R. E. Bird, R. L. Hulstrom and L. J. Lewis, *Sol. Energy, 30* (1983) 563.
6 F. C. Treble, *Proc. Sol. Energy Soc. Conf. C22, London, England, April 1980*, Solar Energy Codes of Practice and Test Procedures, 1980, pp. 1–20.
7 L. J. Reiter, C. S. Borden, J. L. Smith and L. W. Zimmerman, Rating methods for flat-plate and concentrator modules and systems, *Rep. JPLD1805*, Jet Propulsion Laboratory, Pasadena, CA, 1984.
8 Standard method for the calibration and characterization of non-concentrator reference cells under direct normal irradiance, *ASTM Committee E-44.09, Draft 130*, American Society for Testing and Materials, Philadelphia, PA, 1984.
9 Standard methods for the global spectrum calibration of photovoltaic reference cells, *ASTM Committee E-44.09, Draft 178*, American Society for Testing and Materials, Philadelphia, PA, 1984.
10 Standard method for the calibration and characterization of non-concentrator terrestrial photovoltaic reference cells using a tabular spectrum, *ASTM Committee E-44.09, Draft 177*, American Society for Testing and Materials, Philadelphia, PA, 1984.
11 R. J. Matson, K. A. Emery and R. E. Bird, *Sol. Cells, 11* (1984) 105.
12 G. A. Zerlaut, *Proc. Commercial Photovoltaics Measurement Workshop, Vail, CO, July 27–29, 1981, Rep. SERI/CP-214-1403*, Solar Energy Research Institute, Golden, CO, pp. 183–193; *Sol. Cells 7* (1982) 119.
13 D. Bird and R. Hulstrom, Solar Energy Research Institute, 1984.
14 C. R. Osterwald, T. W. Cannon and D. R. Meyers, *Proc. SERI Photovoltaic Adv. Res. Devel. Projects, Golden, CO, October 29–31, 1984, Rep. SERI/CP-211-2507*, Solar Energy Research Institute, Golden, CO.
15 At. T. Chai, *Proc. 2nd Workshop on Terrestrial Photovoltaic Measurements, Baton Rouge, LA, November 10–12, 1976, Rep. ERDA/NASA-1022/76/110*, Energy Research and Development Administration; National Aeronautics and Space Administration, 1976, pp. 233–247.
16 R. E. Bird, *Sol. Energy, 32* (1984) 461.
R. Bird and C. Riordan, Simple solar spectral model for direct and diffuse irradiance

on horizontal and tilted planes at the earth's surface for cloudless atmospheres, *Rep. SERI/TR-215-2436, DE8500 2933*, Solar Energy Research Institute, Golden, CO, 1984.
17 R. Schultz, *IEEE Trans. Instrum. Meas., 26* (1976) 295.
18 L. Castaner, *IEEE Trans. Instrum. Meas., 27* (1978) 152.
19 K. Emery and J. DuBow, *Proc. 14th IEEE Photovoltaic Specialists' Conf., San Diego, CA, January 7-10, 1980*, IEEE, New York, 1980, pp. 506-510.
20 H. Gerwin, Photovoltaic advanced systems test facility: description and operations plan, *SAND 80-1612*, Sandia, NM, 1980.

Appendix A

Nomenclature

A, Area	The total surface area of the electrically active region, including grids and contacts. (For concentrator cells, test cell area is the area designed to be illuminated [1]; for modules and arrays the area is the entire area including frame and borders; for devices that have been mesa etched the area is the area of the junction.)
CN, CN_{STND}	The calibration number expressed in units of (A W^{-1} cm^{-2}) is the short-circuit current divided by the total intensity.
$E_{STND}(\lambda)$	Efficiency η and short-circuit current I_{sc} are measured with respect to the standard spectral irradiance $E_{STND}(\lambda)$.
$E_{TOT}, E_S(\lambda)$	The source spectral (simulated or natural) irradiance.
FOV	The field of view is twice the angle whose tangent is equal to the radius of the limiting aperture divided by the distance between the limiting aperture and receiving aperture in the collimating tube [15]. For a flat plate the FOV is 180°.
I_{sc}	The short-circuit current is the current produced by a device under illumination with less than 20 mV per junction voltage drop across the device.
I_{sc}^{T}	I_{sc} of the test cell measured by the reference cell method.
I_{sc}^{TC}	I_{sc}^{T} corrected for spectral mismatch between $E_{STND}(\lambda)$ and $E_S(\lambda)$, and between $SR_T(\lambda)$ and $SR_R(\lambda)$.
P_{max}	The power at the point on the current-voltage curve when the current-voltage product is a maximum.
M	The spectral mismatch index is used to correct the measured current I_{sc}^{T} to a current with respect to $E_{STND}(\lambda)$ giving I_{sc}^{TC} [A1].
$SR(\lambda)$	Spectral response (A W^{-1}) of a device is the I_{sc} for wavelength λ divided by the incident power.
$SR_R(\lambda)$	Spectral response (A W^{-1}) of the reference cell.
$SR_T(\lambda)$	Spectral response (A W^{-1}) of the test cell.
V_{oc}	The open-circuit voltage is the voltage across the device with no load.
η	The photovoltaic conversion efficiency is P_{max} divided by the intensity. The efficiency is measured with respect to a

standard spectrum, at a standard intensity and temperature (see Appendix B).

Reference for Appendix A

A1 Standard practice for determination of the spectral mismatch parameter between a photovoltaic device and a photovoltaic reference cell, *ASTM Std. E973*, American Society for Testing and Materials, Philadelphia, PA, 1983.

Appendix B

SERI standard solar spectrum

The photovoltaic conversion efficiency is measured with respect to standard reporting conditions as defined by a temperature, intensity and spectrum. One of the first documents defining standard reporting conditions, given in ref. 1, arose out of the second ERDA/NASA photovoltaic measurements workshop held in Baton Rouge, LA in November, 1976. The terrestrial photovoltaic measurement procedures manual in ref. 1 defined the test temperature to the 28 ± 2 °C, intensity to be 100 mW cm^{-2} and gave a tabular standard spectrum. This manual also gave definitions for the area, I_{sc}, V_{oc}, P_{max} and efficiency η which are given in Appendix A. This manual has served as a guide for standard reporting conditions for the United States and many other nations until recently (1984). An updated version of the spectrum in ref. 1 is given in Table B1 and Fig. B1.

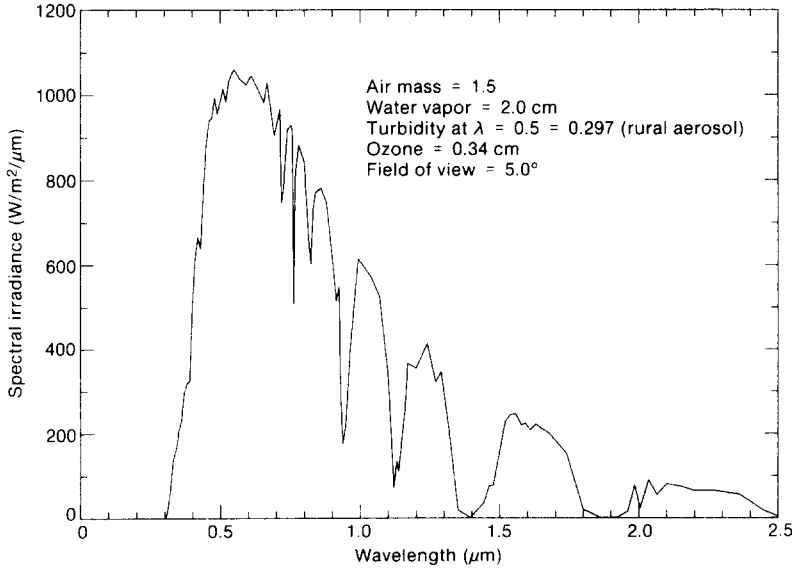

Fig. B1. Standard solar spectrum generated with the BRITE Monte Carlo Solar Insolation Model [5] using the atmospheric conditions specified in ref. 1.

TABLE B1

SERI direct normal standard solar spectrum generated using the model in ref. 5 and the atmospheric conditions specified in ref. 1

λ (μm)	$E(\lambda)$ (W m^{-2} μm^{-1})	λ (μm)	$E(\lambda)$ (W m^{-2} μm^{-1})	λ (μm)	$E(\lambda)$ (W m^{-2} μm^{-1})
0.3050	3.1580	0.7400	918.7104	1.497	147.9616
0.3100	14.4962	0.7525	929.4301	1.520	228.3193
0.3150	37.7810	0.7575	915.1749	1.539	245.2932
0.3200	62.1442	0.7625	509.4725	1.558	246.3954
0.3250	96.7961	0.7675	807.3710	1.578	219.7744
0.3300	135.5833	0.7800	882.2700	1.592	224.8414
0.3350	149.9577	0.8000	842.3254	1.610	208.1645
0.3400	160.9447	0.8160	657.5800	1.630	222.3259
0.3450	177.1257	0.8237	602.8073	1.646	213.5835
0.3500	203.5833	0.8315	729.2128	1.678	200.0180
0.3600	231.7225	0.8400	770.9243	1.740	152.3950
0.3700	295.4179	0.8600	780.7343	1.800	19.9102
0.3800	319.2708	0.8800	745.6021	1.860	0.7584
0.3900	324.8987	0.9050	587.8000	1.920	0.4331
0.4000	499.6553	0.9150	514.7137	1.960	15.0267
0.4100	613.2123	0.9250	548.6353	1.985	78.1094
0.4200	665.5540	0.9300	291.4321	2.005	23.1650
0.4300	639.5195	0.9370	176.2254	2.035	90.4240
0.4400	775.6440	0.9480	220.7315	2.065	55.1248
0.4500	883.9969	0.9650	406.3011	2.100	80.7869
0.4600	938.3870	0.9800	515.6403	2.148	74.9506
0.4700	945.7679	0.9935	614.3025	2.198	64.5313
0.4800	993.0389	1.0400	571.2589	2.270	64.5413
0.4900	955.9850	1.0700	525.1187	2.360	56.0073
0.5000	984.1429	1.1000	338.7496	2.450	16.4662
0.5100	1014.542	1.1200	71.3261	2.500	3.1983
0.5200	983.2030	1.1300	134.5456	2.600	0.0
0.5300	1029.811	1.1370	110.2095	2.700	0.0
0.5400	1049.615	1.1610	266.7685	2.800	0.0
0.5500	1060.333	1.1700	366.3132	2.900	0.4620
0.5700	1037.444	1.2000	354.5366	3.000	2.3180
0.5930	1023.905	1.2400	414.3466	3.100	3.7528
0.6100	1045.908	1.2700	322.0361	3.200	3.7528
0.6300	1020.254	1.2900	346.6621	3.300	2.5854
0.6560	981.5062	1.3200	197.3559	3.400	6.6424
0.6676	1028.718	1.3500	17.9717	3.500	10.2515
0.6930	905.5516	1.3950	0.4832	3.600	9.7459
0.7130	965.6208	1.4425	35.9917	3.700	0.1363
0.7180	746.8997	1.4625	76.7242	3.800	8.6821
0.7244	771.6787	1.4770	77.4871	3.900	7.9258
				4.000	8.0698

In 1983 a standard test method for measuring the electrical performance of non-concentrator terrestrial photovoltaic cells using reference cells was released by the ASTM [B1]. This standard test method describes

standard reporting conditions, equipment, terminology, measurement procedures, translation equations and sources of inaccuracy [B1]. The standard reporting conditions in ref. B1 are different from ref. 1 in the temperature 25 °C *versus* 28 °C and spectrum; ref. 1 *versus* refs. 2 and 3. The Commission of the European Communities (CEC) [B2] and International Electro-Technical Commission (IEC) [B3] have also been involved in developing documents for standard reporting conditions similar to ref. B1.

A significant deviation from standard reporting conditions has occurred in the literature in terms of the definition of the area. The area definition in Appendix A is consistent with the various proposed and adopted test procedures; however, many researchers prefer to report the efficiency based upon the "active" area. The term "active" area is ambiguous because different groups define it differently; however, it usually means the total area (Appendix A) minus an area shadowed by metallization. There can be a substantial difference between the total and active area which can make a device or array with poorly designed metallization appear to be as good as a properly designed device. The issue of what is the area for efficiency measurements will probably remain unresolved for some time since there is political and economic pressure on the various researchers to obtain as high an efficiency as possible.

The Photovoltaic Devices and Measurements Branch at SERI will be adopting the standard reporting conditions recommended by refs. B1 and B3. It is believed that the proposed global spectrum in ref. B4 will be adopted as a standard by the PV community, in which case the Photovoltaic Devices and Measurements Branch will also adopt ref. B4 as a standard spectrum.

References for Appendix B

B1 Standard test methods for electrical performance of non-concentrator terrestrial photovoltaic cells using reference cells, *ASTM Std. E948*, 1983 (American Society for Testing and Materials, Philadelphia, PA).

B2 Standard procedures for terrestrial PV measurements, *CEC Std. 101, Issue 2, EURMO78EN*, 1981 (Commission of the European Communities, Ispra).

B3 Measurement principles for terrestrial photovoltaic solar devices with reference spectral irradiance data, International Electrotechnical Commission, TC82, PV Energy Systems, under consideration, 1986.

B4 R. Hulstrom, R. Bird and C. Riordan, *Sol. Cells, 15* (1985) 365. (An updated version of refs. 2, 3 and 5.)

Appendix C

Spectral mismatch correction to I_{sc}

If the relative spectral response of the reference cell $SR_R(\lambda)$, relative response of the test cell $SR_T(\lambda)$, and the relative spectral irradiance of the source spectrum $E_S(\lambda)$ can be measured, then the spectral mismatch M can be computed as follows [A1, C1]

$$M = \frac{\int_0^\infty SR_R(\lambda)\, E_{STND}(\lambda)\, d\lambda}{\int_0^\infty SR_R(\lambda)\, E_S(\lambda)\, d\lambda} - \frac{\int_0^\infty SR_T(\lambda)\, E_S(\lambda)\, d\lambda}{\int_0^\infty SR_T(\lambda)\, E_{STND}(\lambda)\, d\lambda} \quad \text{(C1)}$$

M is a measure of the fractional error in the current due to the reference cell and source spectrum. The short-circuit current of the test cell (I_{sc}^{T}) can be corrected for spectral mismatch errors to give I_{sc}^{TC} using

$$I_{sc}^{TC} = I_{sc}^{T}/M \quad \text{(C2)}$$

The usefulness of eqn. (C2) to reduce the error in I_{sc}^{T} was evaluated using the reference cells described in Appendix D. Since the reference cells were calibrated in pairs the fractional error between the calibrated value and value obtained using the other cell as a reference cell could be determined. These same pairs of cells were then evaluated indoors with a Spectrolab X-25 solar simulator (Fig. C1) and the fractional error in I_{sc} with and without a correction for spectral mismatch could be determined [C2]. These results are summarized in Table C1. With the exception of SO5 ($CdZnS/CuInSe_2$), outdoor measurements resulted in lower errors. The use of eqn. C2) to correct for spectral mismatch reduced the error in I_{sc} to less than 1% for outdoor measurements and less than 2% for indoor measurements [C1, C2]. The error could be reduced even further when the spectral response of the

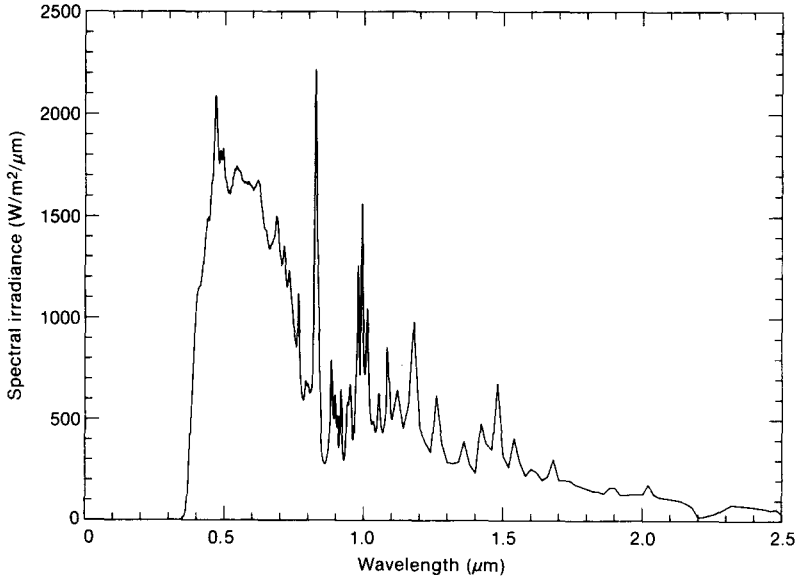

Fig. C1. Typical measured spectral irradiance of SERI's Spectrolab X-25 solar simulator.

TABLE C1

The spectral mismatch index M is used to reduce the error in indoor and outdoor measurements of I_{sc} using the reference cell method. M was computed using the $E_{STND}(\lambda)$ in Table B1

Test cell	*Ref. cell*	*Outdoors*			*Spectrolab X-25*		
		M	*%Error*		*M*	*%Error*	
			I_{sc}^{T}	I_{sc}^{TC}		I_{sc}^{T}	I_{sc}^{TC}
Y225	Y265	0.99787	−0.17	0.04	0.99848	−0.63	−0.48
SO8	Y265	1.01743	1.62	−0.09	0.97672	−3.35	−1.05
Y225	ZO1	0.99518	−0.53	−0.05	0.99591	−1.47	−1.06
Y265	ZO1	0.99720	0.31	0.59	0.99743	−1.16	−0.90
SO2	ZO1	1.0006	−0.03	−0.09	0.98809	−1.25	−0.06
SO4	ZO1	1.0008	0.12	0.04	1.0119	0.10	−1.08
SO4:KG1	ZO1	1.0795	7.79	−0.15	1.1562	15.81	0.16
SO5	ZO1	0.94199	−5.26	0.56	0.99037	−2.63	−1.68
SO8	ZO1	1.0114	0.84	−0.29	1.0212	2.32	0.20
SO5	SO4	0.95374	−4.78	0.07	1.0217	2.70	0.52

test and reference cell were similar. A filtered single crystal silicon cell was used to simulate an amorphous silicon cell's spectral response (SO4:KG1) since amorphous silicon cells tend to be unstable. Testing an amorphous cell indoors or outdoors with a single crystal silicon reference cell can lead to large errors (10%–20%). These errors in I_{sc}^{T} can be reduced to below 1% when corrected for spectral mismatch. Measuring I_{sc}^{T} for any cell outdoors using a black body detector such as a global pyranometer to monitor the intensity will increase the error in I_{sc}^{T} since the reference cell (pyranometer) has a flat spectral response and hence a large spectral mismatch will exist between the reference cell and test cell.

References for Appendix C

C1 C. R. Osterwald and K. A. Emery, *Proc. SERI Polycrystalline Thin Film Review Meeting, Golden, CO, October 24-26, 1984, Rep. SERI/CP-211-2548*, Solar Energy Research Institute, Golden, CO, 1984.

C2 K. Emery, C. Osterwald, T. Cannon, D. Myers, J. Burdick, T. Glatfelter, W. Czubatyj and J Yang, *Proc. 18th IEEE Photovoltaic Specialists' Conf., Las Vegas, NV, October 21-25, 1985*, IEEE, New York, 1985, pp. 623-628.

Appendix D

Summary of reference cell calibrations

The spectral response of a representative sample of eight of the 21 primary reference cells is shown in Figs. D1–D4. These cells represent single crystal silicon cells with different spectral responses, a single crystal GaAs,

thin film Cd(Zn)S/$CuInSe_2$, and CdS/CdTe solar cells. A filtered high efficiency silicon solar cell (SO4:KG1) was used to simulate the spectral response of an amorphous silicon solar cell. All cells were mounted in a package [D1] with a sealed quartz cover plate. Voltage, current and thermo-

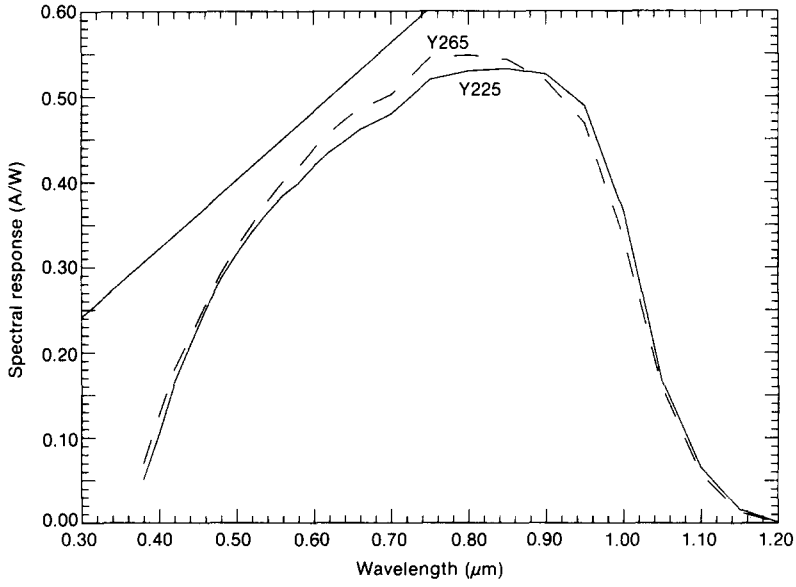

Fig. D1. Spectral response of silicon reference cells Y225 and Y265 showing the unity quantum efficiency line.

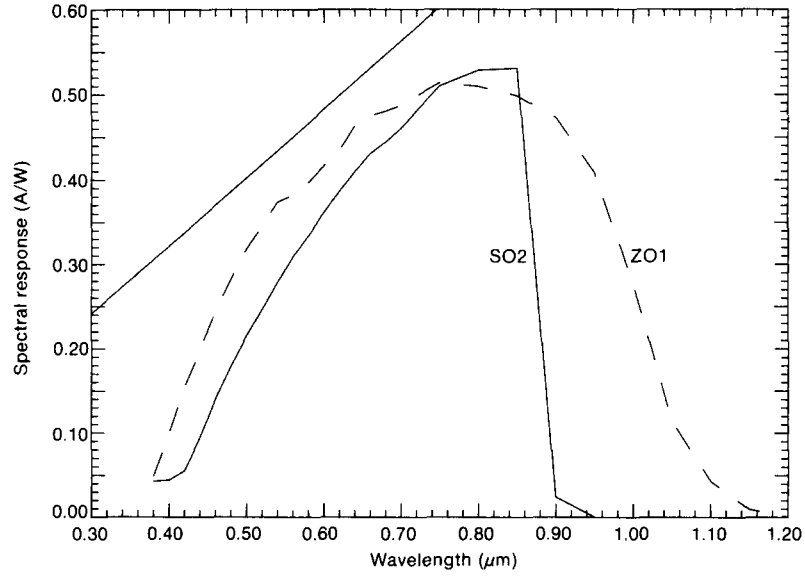

Fig. D2. Spectral response of the silicon reference cell ZO1 and GaAs reference cell SO2.

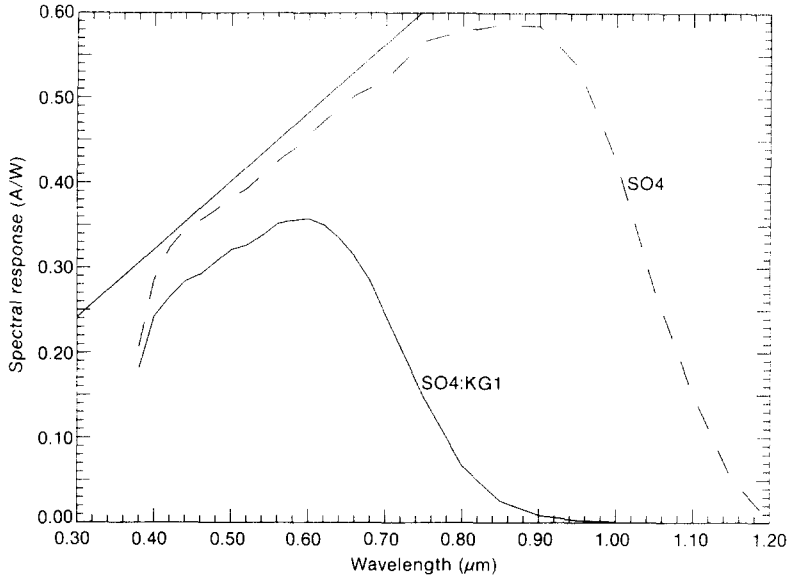

Fig. D3. Spectral response of a high efficiency (17%) single crystal silicon reference cell SO4 and the same cell with a Schottky KG1 filter to simulate the spectral response of an amorphous silicon solar cell.

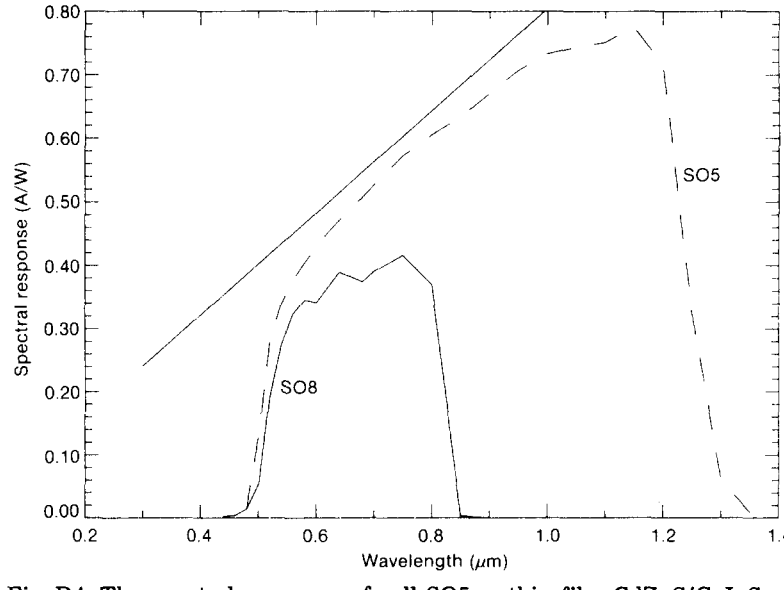

Fig. D4. The spectral response of cell SO5, a thin film CdZnS/$CuInSe_2$ solar cell with a silicon monoxide antireflection coating. Cell SO8 is a thin film CdS/CdTe solar cell.

couple contacts to the cell were made with silver epoxy. Table D1 summarizes the calibration of the eight reference cells (Figs. D1-D4) with respect to the spectrum in Table B1. The use of eqn. (5) to correct the calibration number reduced the standard deviation of the mean calibration

TABLE D1

Summary of reference cell calibrations with respect to spectrum in Table B1 [14]

Cell	*Type*	*Eqn. (3) uncorrected*		*Eqn. (5) corrected*		
		$\langle CN \rangle$ (A W^{-1} cm^{-2})	*Standard deviation* (%)	$\langle CN_{SIND} \rangle$ (A W^{-1} cm^{-2})	*Standard deviation* (%)	*Number of measurements*
Y225	Si(NASA)	1.2129	0.81	1.1920	0.32	15
Y265	Si(NASA)	1.3456	0.70	1.3299	0.29	18
ZO1	Si(NASA)	1.0624	0.52	1.0458	0.15	17
SO2	GaAs	0.8209	1.24	0.7990	0.26	15
SO4	Si	1.3434	0.55	1.3169	0.27	15
SO4 : KG1	Filtered Si	0.5936	1.69	0.5479	0.41	14
SO5	$CdZnS/CuInSe_2$	0.3475	1.68	0.3573	0.68	15
SO8	CdS/CdTe	0.9438	1.08	0.09162	0.26	7

TABLE D2

Summary of reference cell calibrations with respect to various standard spectra using eqn. (5)

Cell	*Type*	*Calibration number* $\langle CN_{STND} \rangle$ (A W^{-1} cm^{-2})					
		Direct[a] [14]	*Direct*[b] [1]	*Direct* [D1]	*Global* [B4]	*Direct*[c] [4]	*Global*[d] [6]
Y225	Si(NASA)	1.192	1.210	1.180	1.188	1.216	1.226
Y265	Si(NASA)	1.330	1.366	1.316	1.329	1.358	1.372
ZO1	Si(NASA)	1.046	1.077	1.035	1.046	1.069	1.081
SO2	GaAs	0.799	0.837	0.787	0.798	0.817	0.818
SO4	Si	1.317	1.352	1.305	1.325	1.345	1.384
SO4:KG1	Filtered Si	0.548	0.592	0.540	0.590	0.569	0.652
SO5	$CdZnS/CuInSe_2$	0.357	0.353	0.355	0.339	0.357	0.334
SO8	CdS/CdTe	0.0916	0.0980	0.0899	0.0914	0.0939	0.0933

[a]See Table B1.
[b]Thekakera.
[c]Japan.
[d]RAE.

number $\langle CN_{STND} \rangle$ to a level $< 1\%$. The silicon reference cells were the least sensitive to $E_S(\lambda)$ being different from $E_{STND}(\lambda)$ while the psuedo-amorphous silicon reference cell (SO4:KG1) was the most sensitive. Table D2 summarizes the calibration number of the eight reference cells (Figs. D1–D4) with respect to various standard spectra using eqn. (5). The spectra given in refs. 1, 4 and 6 are zero in wavelength regions where the terrestrial irradiance is non-zero. This will introduce an offset in the calibration number, giving a calibration number larger than a more realistic solar spectrum generated with the same atmospheric conditions would give. The calibration number for silicon is not very sensitive to the choice of direct normal or global standard spectra. The calibration number for amorphous silicon is about 10% higher for global compared with direct normal, while the calibration number for $Cd(Zn)S/CuInSe_2$ is about 5% lower for global compared with direct normal.

Reference for Appendix D

D1 V. G. Weizer, *Proc. 2nd Workshop on Terrestrial Photovoltaic Measurements, Baton Rouge, LA, November 10–12, 1976*, in *Rep. ERDA/NASA-1022/76/4*, Energy Research and Development Administration; National Aeronautics and Space Administration.
Specification for physical characteristics of non-concentrator terrestrial photovoltaic reference cells, *ASTM E-44.09, E1040-84*, American Society for Testing and Materials, Philadelphia, PA, 1984.